

# Quantification of the Seabed Acoustic Backscatter from a Single-Beam Echosounder Using Sonar5-Pro

Baigo Hamuna<sup>1,2</sup>, Sri Pujiyati<sup>2</sup>, Jonson Lumban Gaol<sup>2</sup>, Totok Hestirianoto<sup>2</sup>

The aim of this study was to quantify and analyze the acoustic backscatter energy reflected from different types of seabeds, including bare sand, seagrass sand, hard corals (massive, branched, and rubble) and soft corals. The acoustic backscatter energy recording was carried out in stationary position using a Simrad EK15 single-beam echo sounder with a frequency of 200 kHz by placing the transducer in a pipe frame. Sonar5-Pro software was used to quantify the acoustic backscatter energy of the seabed and export it for further analysis. The results show that the acoustic backscatter energy differs depending on the type of seabed, e.g. bottom detection energy, bottom peak, attack energy (indicating the hardness of the seabed), decay energy (indicating the roughness of the seabed) and cumulative energy. The acoustic backscattered sound energy decreased at the second and third echo. There are differences in the acoustic wave propagation patterns between different types of seabed, which are reflected in the echo envelope curve, especially in the decay phase, which is highly dependent on the roughness of the seabed surface. Shallow sand forms a curve with a sharper and narrower slope in the decay phase, while corals form a broad curve in the decay phase. The different types of stony corals also show considerable differences in acoustic energy during the decay phase. Massive corals (CM) form broad curves in the decay phase near the top of the echo, while branching corals (ACT and ACB) are at the lower end of the curve. Similarly, the presence of seagrass on the surface affects the hardness level and lowers the energy of bottom detection. Overall, bare sand consistently exhibited a higher bottom peak and attack energy. However, massive corals (CM) have higher bottom detection and decay energy than other seabed types. The difference in acoustic backscatter energy may provide information about seabed characteristics.

## KEYWORDS

- ~ Acoustic backscatter
- ~ Attack and decay phase
- ~ Bottom detection
- ~ Bottom peak
- ~ Simrad EK15
- ~ Sonar5-Pro software

<sup>1</sup> Cenderawasih University, Department of Marine Science and Fisheries, Jayapura City, Indonesia

<sup>2</sup> IPB University, Department of Marine Science and Technology, Bogor, Indonesia

e-mail: [bhamuna@yahoo.com.sg](mailto:bhamuna@yahoo.com.sg)

doi: 10.7225/toms.v14.n01.009

Received: 6 Feb 2024 / Revised: 13 Feb 2025 / Accepted: 3 Mar 2025 / Published: 20 Apr 2025

This work is licensed under



## 1. INTRODUCTION

In general, each type of seabed has different characteristics. These different characteristics influence the strength and weakness of the seabed in reflecting acoustic waves. The acoustic response of the seabed is strongly influenced by the scattering at the water-sediment interface and the amount of backscattering originating from sediment grains, shell debris, and infauna species on the seabed (Thermo et al, 1988; Fonseca and Mayer, 2007; Freitas et al, 2008; Demer et al, 2009; Hamouda and Abdel-Salam, 2010; Hamuna et al, 2018). The reflection and backscattering effects of the seabed are very complex, as it consists of different layers with different compositions (Urlick, 1983). Therefore, acoustic backscatter data are essential for distinguishing seabed types (Manik, 2012; Huang et al., 2018; Amiri-Simkooei et al., 2019).

A single- beam echo sounder (SBES) is a hydroacoustic instrument that can be used to detect seabeds types (Anderson et al., 2008; Poulain et al., 2011). SBES has several advantages in seabed surveys, as echoes from the second bottom can also be integrated into the seabed classification (Penrose et al., 2005; Anderson et al., 2008; Parnum et al., 2009). SBES also has advantages in terms of efficiency and standard data processing procedures, relative ease of instrument operation and high accuracy of results (Anderson et al., 2008; Hilgert et al., 2016). Acoustic backscatter data from SBES have been widely used to determine seabed properties (Manik, 2012; Hamuna et al., 2014; Hilgert et al., 2016; Solikin et al., 2018; Fauziyah et al., 2020; Elson et al., 2022) and for seabed classification and mapping (Bejarano et al., 2010; Mamede et al., 2015; Lee and Lin, 2018; Hamouda et al., 2019; Yusop et al., 2021).

The choice of software for processing and interpreting hydro-acoustic recorded data is a key factor for the user, regardless of the type of SBES instrument used (Hilgert et al., 2016). The two most widely used commercial software for processing SBES data are QTC View Series and RoxAnn System, each taking a different approach. The QTC View software extracts only the shape and energy parameters of the first echo reflected from the seabed. In contrast, the RoxAnn software can extract and analyze the energy of a portion of the first echo reflected from the seabed and all second echoes reflected from the seabed (Poulain et al., 2011).

Sonar5-Pro, developed by Balk and Lindem (2015), applies a method for classifying the hardness and roughness of the seabed based on the theory proposed by Burczynski (1999) in which the echo signal is divided into two parts, namely the energy covering the attack phase (duration: one pulse length from the detection point on the seabed) and the energy covering the decay phase (duration: three pulse lengths from the end of the attack phase). The Sonar5-Pro software is a tool with good capacity for processing acoustic data (Poulain et al., 2011; Zhang et al., 2016; Hilgert et al., 2016, 2019). A Seabed Classification module in the Sonar5-Pro software is useful for quantifying the acoustic backscatter values of the seabed and can export the echo energy reflected from the seabed up to the third echo (Balk and Lindem, 2015). Therefore, Sonar5-Pro can provide information on the acoustic backscatter energy in the upwelling and downwelling phase up to the third echo.

Until now, no research has documented the acoustic backscattered energy in the attack and decay phases up to the third echo reflected by different seabeds (e.g., sand, sand dan vegetation, hard coral, and soft coral). Seabed characteristics from documented SBES detection results only describe acoustic backscatter on the first and second echoes or only from the energy of the first echo. We assume that (1) if the hydro-acoustic recording is carried out in shallow waters, it will be possible to obtain acoustic data up to the third echo, and (2) each seabed type will have different characteristics, not only in the first and second echoes but also in the third echo. Therefore, this study aimed to quantify the acoustic backscatter in the first, second, and third echoes reflected by various types of seabeds, such as sand, sand and seagrass, hard coral, rubble, and soft coral. For this purpose, the solution is to use Sonar5-Pro software because it can quantify and export seabed acoustic backscatter values in the attack and decay phases up to the third echo.

## 2. MATERIALS AND METHODS

### 2.1. Hydro-acoustic Data Acquisition

Hydroacoustic data recording was conducted in May 2023 on Wangi-Wangi Island and Kapota Island, Wakatobi Regency, Southeast Sulawesi Province, Indonesia. The hydroacoustic recordings were conducted at ten stationary points (Figure 1). The instrument used to record the hydroacoustic data was the SBES Simrad EK15 scientific echo sounder (Table 1).

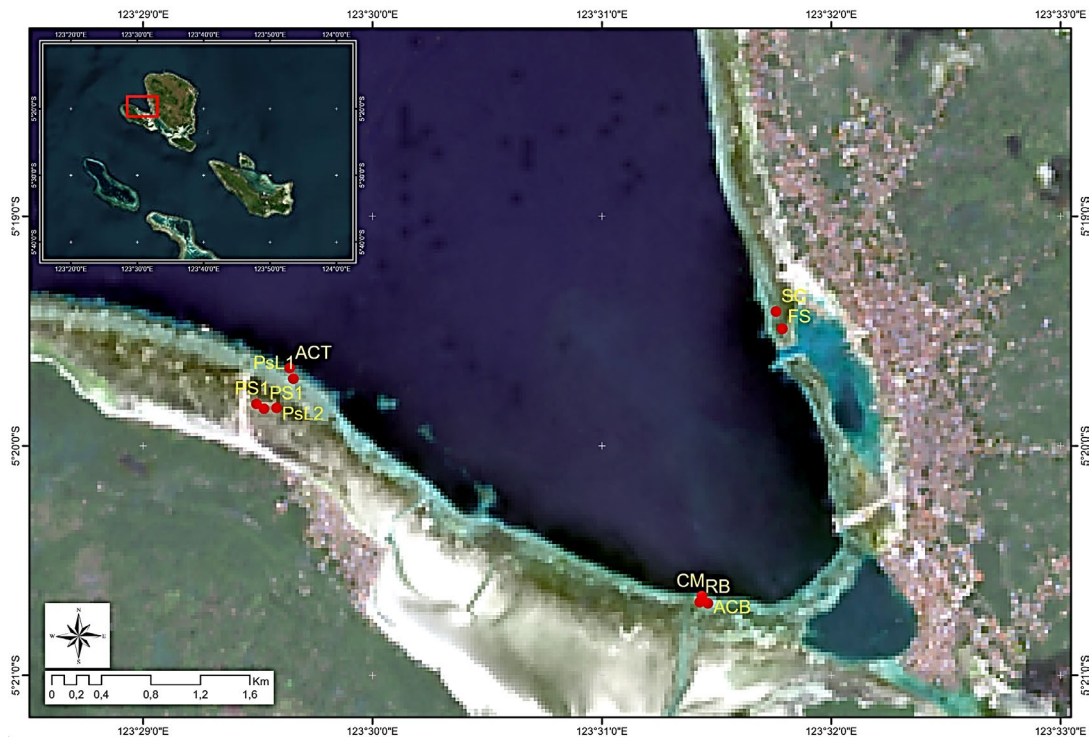


Figure 1. Research location map (stationary acoustic data acquisition).

Parameters	Description
Transducer type	Single beam
Frequency	200 kHz
Beam width	26°
Ping rate	>40 Hz
Pulse length	0.16 ms
Pulse duration	80 – 1240 $\mu$ s
Output power	45 W

Table 1. SBES Simrad EK15 scientific echosounder specifications (Source: Simrad, 2012).

The hydroacoustic data recording was stationary for 5 to 10 minutes. During the recording, the transducer was installed in a frame made of PVC pipe to facilitate the recording of acoustic data and to protect the transducer from the influence of waves (Figure 2). The transducer was aligned vertically and perpendicular to the target. The hydroacoustic recording began by recording the acoustic reflection of a 35 mm diameter sphere (target strength, TS: -45.96 dB) to calibrate the instrument. The results showed that the TS value of the sphere was -47.09 dB, which is close to the actual TS value. Acoustic backscatter recordings were then made of eight types of seabeds, including sand (SA), sand and seagrass (SaSg) and hard corals (Acropora tabulate; ACT, Acropora branching; ACB, Coral massive; CM, Coral foliose; CF, rubble; RB and soft corals; SC) (Figure 3). Oceanographic parameters such as salinity, temperature and pH of seawater were also measured and used for the calibration process during data processing.

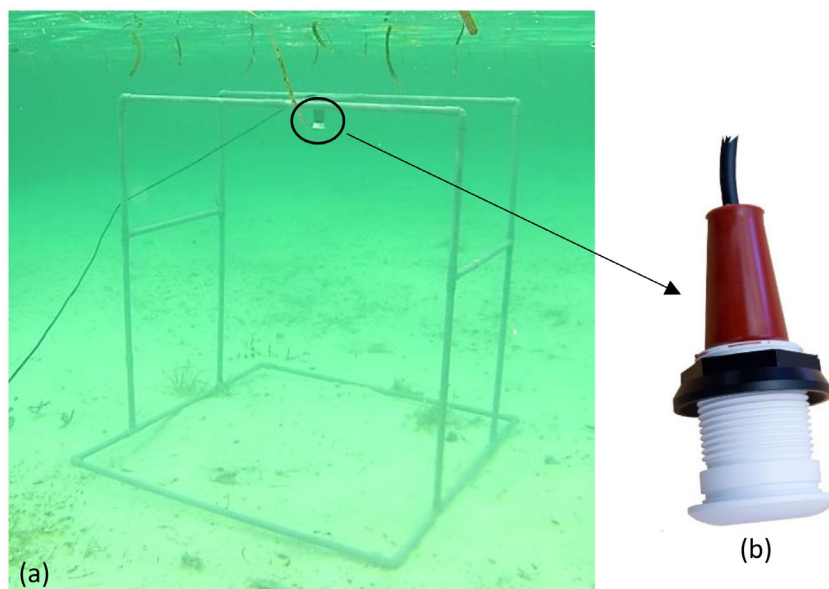


Figure 2. (a) Frame used for acoustic data recording, and (b) Simrad EK15 transducer.

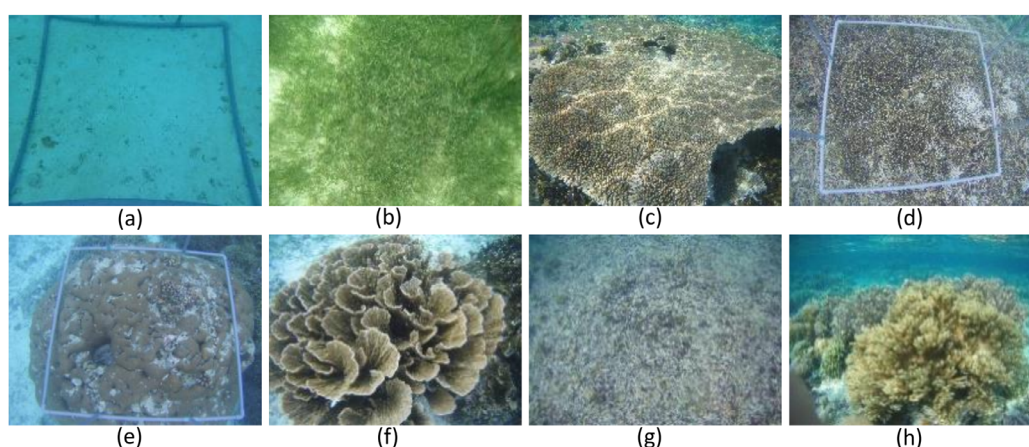


Figure 3. The type of seabed that is the target for acoustic backscatter recording: (a) sand (SA), (b) sand and seagrass (SaSg), (c) *Acropora tabulate* (ACT), (d) *Acropora branching* (ACB), (e) *Coral massive* (CM), (f) *Coral foliose* (CF), (g) rubble (RB), and (h) soft coral (SC).

## 2.2. Data Processing

The data processing resulting from the hydroacoustic recordings was carried out using Sonar5-Pro software (Balk and Lindem, 2015). The first step in processing the recorded data is to calibrate the data by entering the values of the oceanographic parameters measured in situ (water temperature, salinity and pH). For the identification of the seabed in the Sonar5-Pro software, there is an analysis tool "Bottom Classification" with three methods to identify the seabed: Best Candidate, Image Analysis and Bottom Up (Balk and Lindem, 2015). In this study, the Best Candidate method was used to automatically recognise the seabed surface. The threshold for detecting the seabed surface is -40 dB (Shao et al., 2021). The minimum depth for seabed detection is 1 m from the water surface and the maximum detection depth is 10 m. Although the Sonar5-Pro software can automatically detect the seabed, re-checking and manual correction is required.

## 2.3. Data Analysis

In the Sonar5-Pro software, many acoustic parameters can be determined from the echo signals reflected from the seabed, from the first, second and third echoes (Figure 4) (Balk and Lindem, 2015). Figure 4 shows the acoustic parameters of the first echo from the seabed, but the same parameters are also present in the second and third echoes. Only five acoustic parameters were analyzed in this study: Bottom Detection (BD), Bottom Peak (BP), Attack Energy (AttackSv), Decay Energy (DecaySv) and Cumulative Energy (AttDecSv). The attack energy is the acoustic energy in the attack phase, which begins when the acoustic wave first hits the seabed (bottom detection) and lasts for the duration of a acoustic wave. The energy of the attack phase is mainly caused by the surface of the seabed and can therefore be used to measure acoustic

hardness or reflectivity. The decay energy is the acoustic energy in the decay phase, which begins after the attack phase and lasts for the duration of three acoustic waves. It is caused by diffuse backscattering from the sediment volume and is strongly dependent on the degree of roughness of the seabed (Burczynski 1999; Balk and Lindem, 2015). The cumulative energy is the acoustic energy resulting from the summation of the energy in the attack and decay phases during the propagation of the acoustic waves in the seabed. The attack, decay and cumulative energy can be found in each echo from the seabed (the first, second and third echoes). Acoustic parameter values from the first seabed (first echo) to the third seabed (third echo) were exported as a .txt file. Subsequently, the erroneous data (value-999) generated from pixels without values were removed before further analysis.

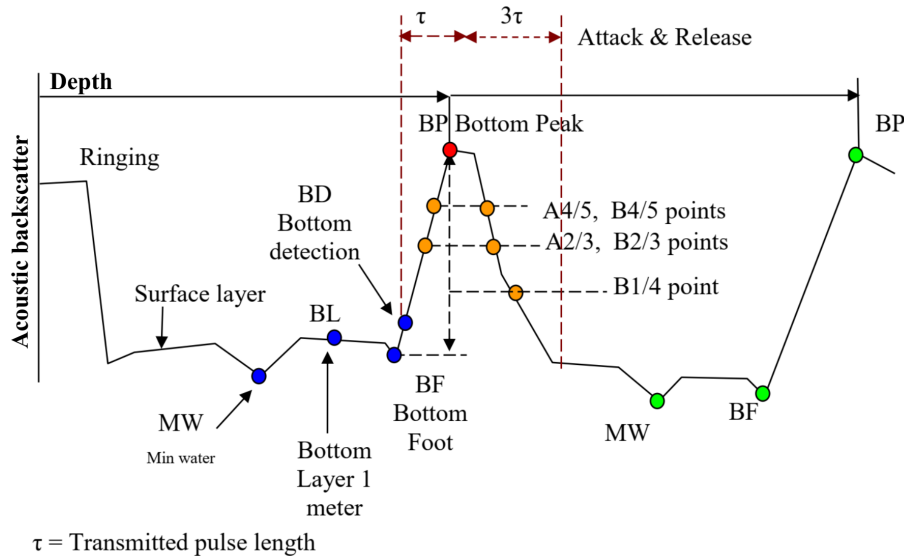


Figure 4. A curve showing acoustic parameters at the first echo of the seabed using Sonar5-Pro software (Source: Balk and Lindem, 2015). The attack phase begins when the acoustic wave first hits the seabed up to the duration of one acoustic wave, while the decay phase begins after the attack phase up to the duration of three acoustic waves.

The attack and decay energies describe the average volume backscattering strength ( $S_v$ ) during the attack or decay phase. To calculate the acoustic backscatter energy during the attack or decay phase ( $AttackS_v$  and  $DecayS_v$ ; dB), the echo energy of each sample must be converted to intensity (linear value), then added and divided by the number of attack or decay samples and converted back to decibel values. Mathematically,  $AttackS_v$  and  $DecayS_v$  can be calculated based on Equations (1) and (2) (Balk and Lindem, 2015):

$$AttackS_{v_x} = 10 \log \left( \frac{1}{N_A} \sum_{i=AI_1}^{AI_2} (10^{S_{v_i}/10}) \right) \quad (1)$$

$$DecayS_{v_x} = 10 \log \left( \frac{1}{N_D} \sum_{i=DI_1}^{DI_2} (10^{S_{v_i}/10}) \right) \quad (2)$$

where,

$$AI_1 = Bottom \ index \quad (3)$$

$$AI_2 = Bottom \ index + Attack \ samples \quad (4)$$

$$DI_1 = Bottom \ index + Attack \ samples + 1 \quad (5)$$

$$DI_2 = Bottom \ index + Attack \ samples + 1 + Decay \ samples \quad (6)$$

where,  $x$  shows the first to third echoes;  $N_A$  and  $N_D$  are the number of attack and decay samples, respectively (Balk and Lindem, 2015).

In addition, this study also calculated the cumulative energy, which represents the total energy of each echo reflected from the seabed (first to third echoes). Based on Equation 7, the cumulative energy ( $AttDecS_v1$ ,  $AttDecS_v2$  and

AttDecSv3) of each echo on the seabed is determined using the energy of the attack and decay phase. The cumulative energy of each echo can be determined by converting the AttackSvX and DecaySvX values into intensity values and then weighting them by the attack and decay samples (NA and ND) according to the following equation (Balk et al., 2011):

$$AttDecSv_x = 10 \log \left( \frac{1}{N_A + N_D} \left( N_A \times 10^{\frac{AttackSv_i}{10}} + N_D \times 10^{\frac{DecaySv_i}{10}} \right) \right) \quad (7)$$

In the Sonar5-Pro software, the number of attack samples (NA) is 8 and the number of decay samples (ND) is 24 (3 times the number of attack samples). When integrating into the DecaySv value, the first attack sample is not used, so the number of decay samples (ND) is 23 (not 24), which must be used to calculate the AttDecSv2 value (Poulain et al., 2011). Equation (7) is also used to calculate the AttDecSv3 value of the third echo energy reflected from the seabed.

## 2.4. Statistical Analysis

In this study, the statistical analysis aimed to determine the significance level of the similarities or dissimilarities of the acoustic backscatter energies between the seabed types in each seabed echo (first, second and third echoes). The statistical analysis used is the Analysis of Variance (ANOVA) in XLSTAT Basic+ software (Lumivero, 2014). Tukey HSD (Honestly Significant Difference) with a confidence interval of 5 % ( $\alpha = 0.05$ ) was used as the test method for the pairwise comparison.

## 3. RESULTS

### 3.1. Echogram and Acoustic Wave Propagation Curve

Each acoustic pulse reflected from the seabed contains information that varies depending on the characteristics of the seabed. The results of the hydroacoustic recordings, which describe the acoustic backscatter strength of the seabed, can be represented in the form of an echogram, which serves as a control in the data analysis (Figure 5). There are three echoes reflected from different layers of the seafloor with different acoustic backscatter strengths (differences in color scale): (1) the first echo, which is a direct reflection echo from the seabed received by the transducer; (2) the second echo, which is from the reflection of the seabed hitting the water surface and reflected from the water surface toward the seabed, then reflected from the seabed (reflected twice from the seabed and once from the water surface); and (3) the third echo, which is an echo reflected three times from the seabed and twice from the water surface.

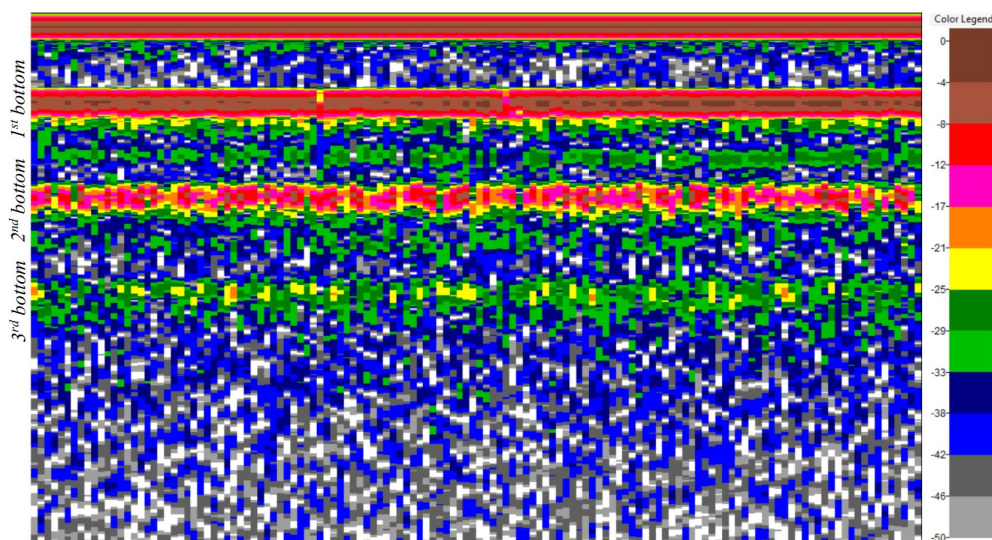


Figure 5. An acoustic backscatter echogram (first to third echoes) was recorded using SBES Simrad EK-15.

Figure 6 shows the propagation of the acoustic wave up to the third echo from the seabed. The acoustic wave propagation curves differ between the different types of seabeds, especially in the decay phase (after the bottom peak). The difference in the shape of the decay phase curve depends strongly on the roughness of the seabed surface. Shallow sand forms a curve in the decay phase that is relatively similar to the attack phase, with a sharper and narrower curve, while corals with branches produce a broader curve in the decay phase. A narrow echo envelope curve has a higher amplitude of acoustic backscattered energy than a broad curve.

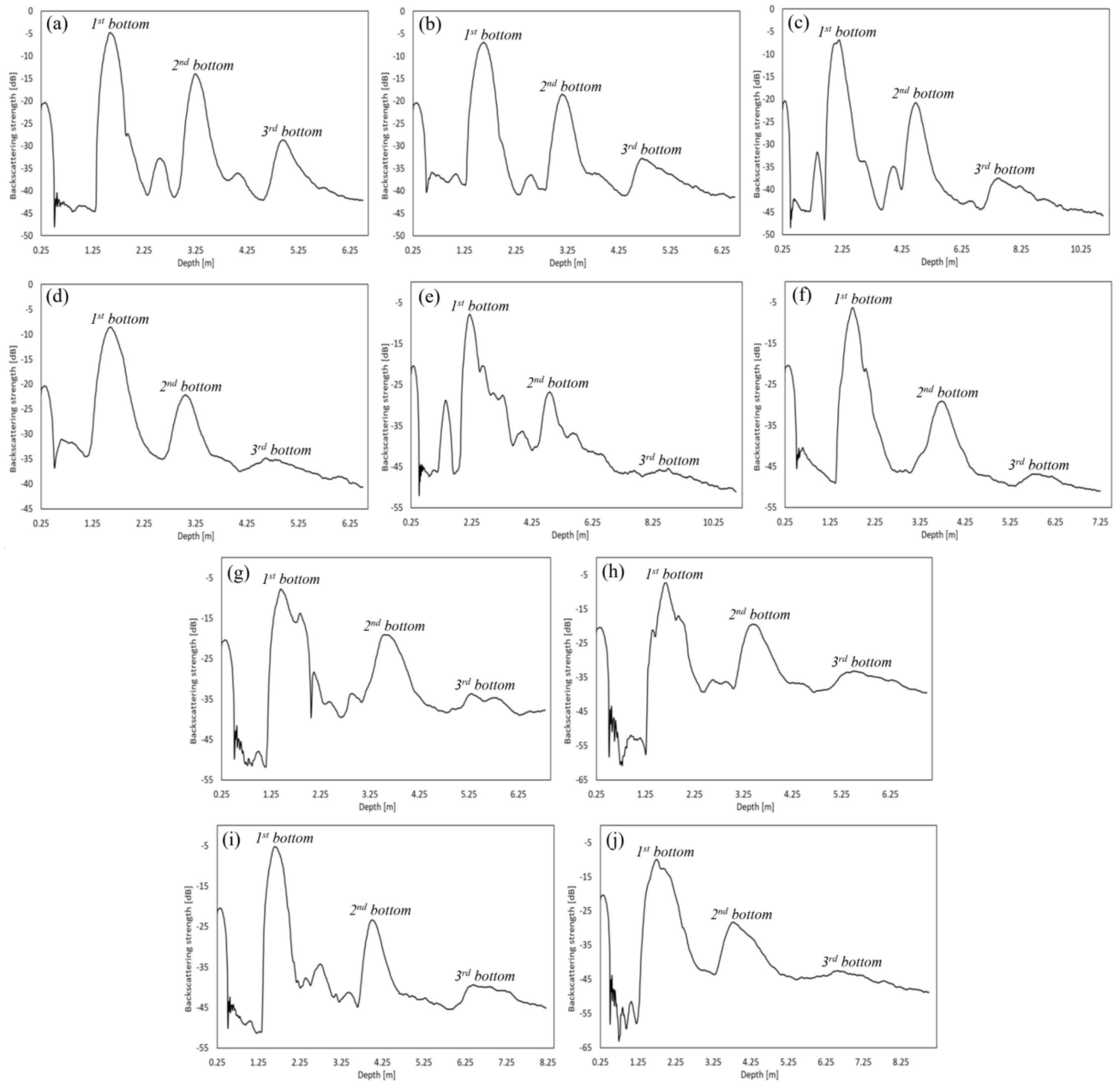


Figure 6. Acoustic wave echo-envelope curve; (a)-(b) sand (SA), (c)-(d) sand and seagrass (SaSg), (e) *Acropora tabulate* (ACT), (f) *Acropora branching* (ACB), (g) *Coral massive* (CM), (h) *Coral foliose* (CF), (i) rubble (RB), and (j) soft coral (SC).

### 3.2. Bottom Detection and Bottom Peak

Table 2 shows that the average bottom detection energy (BD) of CM hard corals was higher than that of other seabed types. This indicates that the CM surface is harder than sand, soft corals and different types of hard corals. The BD energy of all hard corals species is higher than that of soft corals, which is due to the differences in surface structure, as soft corals have a soft and smooth surface. Differences in BD energy also occurred in bare sand (SA) and sand with seagrass on the surface (SaSg). This is likely due to the initial length of the acoustic pulse impinging on the seagrass, so the detected energy was lower than that in bare sand.

Seabed type	BD	BP <sub>1</sub>	BP <sub>2</sub>	BP <sub>3</sub>
SA1	-28.85±2.94	-6.06±0.69	-15.89±4.65	-29.91±3.13
SA2	-28.52±1.85	-6.69±1.26	-18.45±4.18	-31.77±2.34
SaSg1	-30.51±5.76	-8.50±1.32	-22.95±3.14	-38.58±3.49
SaSg2	-30.52±5.32	-9.76±1.73	-22.29±3.50	-35.95±3.15
ACT	-28.22±3.56	-9.35±2.55	-28.19±3.36	-41.57±2.79
ACB	-28.81±4.33	-7.85±1.85	-30.27±3.38	-43.30±2.15
CM	-25.48±2.55	-8.05±0.46	-20.08±3.42	-33.47±3.67
CF	-29.75±3.35	-8.84±1.09	-24.85±3.57	-34.79±2.12
RB	-27.63±2.90	-6.27±0.46	-22.51±3.70	-34.88±4.32
SC	-30.53±2.97	-11.59±2.06	-31.98±2.77	-45.58±3.64

Table 2. Average energy of bottom detection and bottom peak (in decibel units; dB).

The energy of the bottom peak (BP) is different for the three echoes of the seabeds and decreases further for the second and third echoes (Table 2). This is due to various factors, such as the significantly different propagation distances of the sound waves and energy losses due to absorption in the water medium. Although SA and RB have lower BD energy than CM in the first echo, the BP<sub>1</sub> energy of these two seabed types is higher than that of the other types. This is probably due to the fact that the subsurface structure and composition of SA and RB are harder and denser than those of CM and other seabed types. The sub-surface structure and composition of sand grains tend to be denser and harder because they are bound together, so it is not easy to stick a pipe into the seabed when taking sand samples. Also, the RB composition tends to be scattered, so acoustic waves hit the harder parts of the coral sticks.

There are significant differences in BP energy between similar bottom types such as SA and SaSg. In BP<sub>1</sub>, the difference between the two ground types is only about -2 to -3 dB, but the difference increases from -4 to -7 dB in BP<sub>2</sub> and -4 to -8 dB in BP<sub>3</sub>. Similarly, the energy difference in BP<sub>2</sub> and BP<sub>3</sub> between massive corals (CM) and branched corals (ACT and ACB) reached -10 dB. Thus, the surface structure and relief, which are flat, rough or branched, may also influence the high and low energies of BP<sub>2</sub> and BP<sub>3</sub>. Overall, the energy difference from BP<sub>1</sub> to BP<sub>2</sub> ranged from -9.83 to -22.41 dB, while the energy difference from BP<sub>2</sub> to BP<sub>3</sub> ranged from -10.94 to -15.63 dB.

### 3.3. Acoustic Backscattering in the Attack and Decay Phases

The results of quantifying the acoustic backscatter energy for each type of seabed in the attack and decay phases, consisting of the average AttackSv and DecaySv energy for three different echoes, are shown in Table 3. The observed variations in acoustic energy during the attack and decay phases show that each value provides information about the degree of hardness (in the attack phase) and roughness (in the decay phase), which differ between the different seabed types. Higher AttackSv and DecaySv energies indicate a higher degree of hardness or roughness of the seabed. The opposite is true for low AttackSv and DecaySv energies.

In the first echo, sand types (except SaSg2) have a higher AttackSv<sub>1</sub> energy than other seabed types. However, the DecaySv<sub>1</sub> energy of CM was higher than that of all other sand types. This is probably due to the basic structure of each type of seabed. Sand with a dense and hard structure and layers will produce high energy in the attack phase. CM corals, on the other hand, provide high energy in the decay phase because they have a rough surface but a dense and robust structure. Similarly, the AttackSv<sub>1</sub> energy is higher for ACT, ACB and RB types than for CM and CF. However, the DecaySv<sub>1</sub> energy of the three types is lower than that of CM and CF (the DecaySv<sub>1</sub> energy of CF is higher than that of ACB and RB). Although they are both coral types (hard coral: ACB; rubble: RB), there are significant differences in the decay phase after passing the bottom peak. Overall, the cumulative energy (AttDecSv<sub>1</sub>) was higher for the sand type than for the hard and soft corals (Table 4).

SA and CM consistently have higher AttackSv<sub>2</sub> energy on the second echo and AttackSv<sub>3</sub> on the third echo than other seabed types. Similarly, AttDecSv<sub>2</sub> and AttDecSv<sub>3</sub> energies were higher for SA and CM. However, this was not true for DecaySv<sub>2</sub> and DecaySv<sub>3</sub> energies, where CM was higher than SA and other seabed types. Even the DecaySv<sub>3</sub> energy of CF is higher than that of SA. Interestingly, the AttackSv and DecaySv energies were between the two sand types (SA and SaSg). SA has a higher AttackSv energy, but the DecaySv energies for both are relatively the same in the first, second and

third echoes. This may be influenced by the presence of seagrass growth on the surface, which can have a rough effect during the decay phase.

Seabed type	AttackSv <sub>1</sub>	DecaySv <sub>1</sub>	AttackSv <sub>2</sub>	DecaySv <sub>2</sub>	AttackSv <sub>3</sub>	DecaySv <sub>3</sub>
SA1	-9.16±0.83	-21.47±3.64	-17.70±4.54	-31.07±4.33	-30.48±3.33	-37.33±2.57
SA2	-10.61±1.60	-22.39±2.87	-19.93±4.87	-32.94±3.40	-32.23±3.06	-37.37±1.98
SaSg1	-10.93±1.91	-22.06±2.62	-22.21±3.58	-32.26±2.80	-36.54±3.10	-38.86±1.79
SaSg2	-12.12±2.95	-22.98±2.58	-22.45±3.60	-32.71±2.97	-33.99±4.07	-37.82±1.92
ACT	-10.66±2.83	-24.01±2.37	-27.53±3.21	-34.20±2.75	-44.73±3.27	-43.91±2.04
ACB	-11.95±2.11	-28.41±2.50	-29.99±2.98	-34.24±2.94	-40.63±3.03	-38.66±1.97
CM	-12.88±0.73	-21.35±1.66	-19.20±2.33	-28.99±2.93	-32.10±3.48	-35.41±1.93
CF	-12.47±1.08	-24.20±1.52	-24.54±2.93	-32.79±3.35	-37.52±3.87	-36.35±2.00
RB	-10.81±0.56	-26.22±1.46	-24.77±3.23	-31.04±3.12	-36.60±3.00	-38.42±2.06
SC	-12.57±3.00	-28.24±3.05	-28.48±3.41	-35.96±2.50	-43.11±3.80	-42.19±1.97

Table 3. The average energy of acoustic backscatter in the attack and decay phases (in decibels; dB).

Seabed type	AttDecSv <sub>1</sub>	AttDecSv <sub>2</sub>	AttDecSv <sub>3</sub>
SA1	-14.47±0.87	-24.43±4.15	-33.72±2.28
SA2	-16.00±1.50	-25.40±3.49	-35.42±1.72
SaSg1	-16.10±1.60	-25.91±2.75	-38.15±2.07
SaSg2	-16.82±1.79	-27.39±2.73	-35.98±2.33
ACT	-16.22±2.47	-31.75±2.50	-43.87±1.90
ACB	-16.75±1.73	-32.56±2.79	-39.68±1.74
CM	-16.63±0.81	-24.03±2.86	-34.70±2.83
CF	-17.69±0.87	-27.68±3.16	-36.81±2.93
RB	-18.93±0.54	-27.19±3.00	-37.70±2.57
SC	-18.43±2.02	-32.97±2.25	-42.40±2.60

Table 4. Average accumulative energy of acoustic backscatter in the first to third echoes (in decibel units; dB).

### 3.4. Similarity of Acoustic Backscatter Values

The test results of the differences in the average acoustic backscatter values between the seabed types showed that the similarity of the average acoustic backscatter values in the three echoes of the seafloor was 16.89% (first echo), 7.78% (second echo) and 5.00% (third echo) (Tables 5 to 7). In the first echo, the predominant similarity in acoustic backscatter energy was found in the average energies of BD and BP1. SA tended to be similar in average BD with branched corals (ACT and ACB; sig=0.55 and sig=0.88) and RB (sig=0.91). It also has the same BP1 energy with ACB (sig=1.00), RB (sig=0.08) and CF (sig=0.99). SA also has similar AttackSv<sub>1</sub> and DecaySv<sub>1</sub> energies to ACT (sig=0.07 and sig=0.91 respectively). Separately, SA has similarities in several significant acoustic backscatter energies with other seabed types, such as AttackSv<sub>1</sub> energy with RB (sig=1.00) and ACB (sig=0.23), DecaySv<sub>1</sub> energy with CF (sig=0.99), and AttDecSv<sub>1</sub> energy with SaSg (SA1 vs. SaSg1: sig=0.89; SA2 vs. SaSg2: sig=0.64). There were similarities in acoustic backscatter energy between different types of stony corals, such as BD and AttackSv<sub>1</sub> energy (ACT vs. ACB; sig=0.11 and sig=0.99), BP1 energy (ACT vs. CF; sig=1.00), DecaySv<sub>1</sub> energy (ACT vs. CF; sig=1.00), and AttDecSv<sub>1</sub> energy (ACT vs. ACB; sig=0.27, and ACB vs. CM; sig=0.94). The AttDecSv<sub>1</sub> energy of SC was similar to that of different species of hard corals (sig=0.33 to 0.98), except for CF (sig<0.05).

The acoustic backscatter energy between the hard coral species differed considerably in the second echo. Meanwhile, SA shows similarities with SaSg only in DecaySv<sub>2</sub> and AttDecSv<sub>2</sub> energies (sig=0.46 and sig=0.68, respectively), BP2 energy with CM (sig=0.06) and DecaySv<sub>2</sub> energy with CF (sig=1.00). However, SA1 and SA2 show a significant degree

of similarity only for BP2 energy (sig=1.00). Similarly, SaSg1 and SaSg2 only show significant similarity in AttackSv2 energy (sig=0.98). RB is similar to ACB in DecaySv2 (sig=0.95) and CF in AttackSv2 (sig=0.54). For some acoustic backscatter energies, there are similarities between SC and ACT in the second echo, namely the energies of AttackSv2, DecaySv2 and AttDecSv2 (sig=0.39, sig=0.16 and sig=1.00, respectively).

In the third echo, the similarity of BP3 energy occurred only between SaSg2 and CF (sig=0.91). SA1 and SA2 have similar DecaySv3 energy (sig=1.00). Both also have similar DecaySv3 energies to CF (sig=0.62 and sig=0.70). The acoustic backscatter energy of soft corals differs significantly in the third echo from that of other seabed types.

Seabed type			SA2	SaSg1	SaSg2	ACT	ACB	CM	CF	RB	SC	
SA1	BD	Att <sub>1</sub>	=	≠	≠	≠	≠	=	≠	=	≠	≠
	BP <sub>1</sub>	Dec <sub>1</sub>	≠	≠	≠	≠	≠	≠	≠	=	≠	≠
	AttDec <sub>1</sub>		≠	=	≠	≠	≠	≠	≠	≠	≠	≠
SA2	BD	Att <sub>1</sub>		≠	≠	≠	=	=	≠	=	≠	≠
	BP <sub>1</sub>	Dec <sub>1</sub>		≠	≠	≠	=	=	≠	=	≠	≠
	AttDec <sub>1</sub>			≠	=	≠	≠	≠	≠	≠	≠	≠
SaSg1	BD	Att <sub>1</sub>			=	≠	≠	≠	≠	≠	≠	≠
	BP <sub>1</sub>	Dec <sub>1</sub>			≠	≠	≠	≠	≠	=	≠	≠
	AttDec <sub>1</sub>				≠	≠	≠	≠	≠	≠	≠	≠
SaSg2	BD	Att <sub>1</sub>				≠	≠	≠	≠	≠	=	≠
	BP <sub>1</sub>	Dec <sub>1</sub>				=	≠	≠	≠	≠	≠	=
	AttDec <sub>1</sub>					=	≠	≠	≠	≠	≠	≠
ACT	BD	Att <sub>1</sub>					=	=	≠	≠	≠	≠
	BP <sub>1</sub>	Dec <sub>1</sub>					≠	≠	≠	=	≠	≠
	AttDec <sub>1</sub>						=	≠	≠	≠	=	≠
ACB	BD	Att <sub>1</sub>						≠	≠	=	≠	≠
	BP <sub>1</sub>	Dec <sub>1</sub>						≠	≠	≠	≠	≠
	AttDec <sub>1</sub>							=	≠	≠	=	≠
CM	BD	Att <sub>1</sub>							≠	≠	≠	≠
	BP <sub>1</sub>	Dec <sub>1</sub>							≠	≠	=	≠
	AttDec <sub>1</sub>								≠	≠	=	≠
CF	BD	Att <sub>1</sub>								≠	≠	=
	BP <sub>1</sub>	Dec <sub>1</sub>								≠	≠	≠
	AttDec <sub>1</sub>									≠	≠	≠
RB	BD	Att <sub>1</sub>									≠	≠
	BP <sub>1</sub>	Dec <sub>1</sub>									≠	≠
	AttDec <sub>1</sub>										≠	≠

Note: Att is AttackSv; Dec is DecaySv; AttDec is AttDecSv; the ≠ sign indicates significant difference; the = sign indicates there is a similarity

Table 5. Summary of similarity of acoustic backscattered energy in first echo (Tukey HSD; α = 0.05).

Seabed type			SA2	SaSg1	SaSg2	ACT	ACB	CM	CF	RB	SC
SA1	BP <sub>2</sub>	Dec <sub>2</sub>	=	≠	≠	≠	≠	=	≠	≠	≠
	Att <sub>2</sub>	AttDec <sub>2</sub>	≠	≠	≠	≠	≠	≠	≠	≠	≠
SA2	BP <sub>2</sub>	Dec <sub>2</sub>		≠	≠	≠	≠	=	≠	=	≠
	Att <sub>2</sub>	AttDec <sub>2</sub>		≠	=	≠	≠	≠	≠	≠	≠
SaSg1	BP <sub>2</sub>	Dec <sub>2</sub>			≠	≠	≠	≠	=	≠	=
	Att <sub>2</sub>	AttDec <sub>2</sub>			=	≠	≠	≠	≠	≠	≠
SaSg2	BP <sub>2</sub>	Dec <sub>2</sub>				≠	≠	≠	≠	≠	≠
	Att <sub>2</sub>	AttDec <sub>2</sub>				≠	≠	≠	≠	≠	≠
ACT	BP <sub>2</sub>	Dec <sub>2</sub>					≠	≠	≠	≠	≠
	Att <sub>2</sub>	AttDec <sub>2</sub>					≠	≠	≠	≠	=
ACB	BP <sub>2</sub>	Dec <sub>2</sub>						≠	≠	≠	≠
	Att <sub>2</sub>	AttDec <sub>2</sub>						≠	≠	≠	≠
CM	BP <sub>2</sub>	Dec <sub>2</sub>							≠	≠	≠
	Att <sub>2</sub>	AttDec <sub>2</sub>							≠	≠	≠
CF	BP <sub>2</sub>	Dec <sub>2</sub>								≠	≠
	Att <sub>2</sub>	AttDec <sub>2</sub>								=	≠
RB	BP <sub>2</sub>	Dec <sub>2</sub>									≠
	Att <sub>2</sub>	AttDec <sub>2</sub>									≠

Note: Att is AttackSv; Dec is DecaySv; AttDec is AttDecSv; the ≠ sign indicates significant difference; the = sign indicates there is a similarity

Table 6. Summary of similarity of acoustic backscattered energy in second echo (Tukey HSD; α = 0.05).

Seabed type			SA2	SaSg1	SaSg2	ACT	ACB	CM	CF	RB	SC
SA1	BP <sub>3</sub>	Dec <sub>3</sub>	≠	=	≠	≠	≠	≠	≠	=	≠
	Att <sub>3</sub>	AttDec <sub>3</sub>	≠	≠	≠	≠	≠	≠	≠	≠	≠
SA2	BP <sub>3</sub>	Dec <sub>3</sub>		≠	≠	≠	≠	≠	≠	=	≠
	Att <sub>3</sub>	AttDec <sub>3</sub>		≠	≠	≠	≠	≠	≠	≠	≠
SaSg1	BP <sub>3</sub>	Dec <sub>3</sub>			≠	≠	≠	=	≠	≠	≠
	Att <sub>3</sub>	AttDec <sub>3</sub>			≠	≠	≠	≠	≠	≠	≠
SaSg2	BP <sub>3</sub>	Dec <sub>3</sub>				≠	≠	≠	=	=	≠
	Att <sub>3</sub>	AttDec <sub>3</sub>				≠	≠	≠	≠	≠	≠
ACT	BP <sub>3</sub>	Dec <sub>3</sub>					≠	≠	≠	≠	≠
	Att <sub>3</sub>	AttDec <sub>3</sub>					=	≠	≠	≠	≠
ACB	BP <sub>3</sub>	Dec <sub>3</sub>						≠	≠	≠	≠
	Att <sub>3</sub>	AttDec <sub>3</sub>						≠	≠	≠	≠
CM	BP <sub>3</sub>	Dec <sub>3</sub>							≠	≠	≠
	Att <sub>3</sub>	AttDec <sub>3</sub>							≠	≠	≠
CF	BP <sub>3</sub>	Dec <sub>3</sub>								≠	≠
	Att <sub>3</sub>	AttDec <sub>3</sub>								≠	≠
RB	BP <sub>3</sub>	Dec <sub>3</sub>									≠
	Att <sub>3</sub>	AttDec <sub>3</sub>									≠

Note: Att is AttackSv; Dec is DecaySv; AttDec is AttDecSv; the ≠ sign indicates significant difference; the = sign indicates there is a similarity

Table 7. Summary of similarity of acoustic backscattered energy in third echo (Tukey HSD; α = 0.05).

#### 4. DISCUSSION AND CONCLUSION

The difference in acoustic backscatter from different types of seabed provides information about the properties of the seabed at the surface and below the surface (Chotiros, 2017; Brown et al., 2019). A hard seabed produces a sharp echo envelope curve, while a soft seabed produces a rising curve with a relatively low slope (Burczynski, 1999; Boulton and Wyness, 2001; Hamilton, 2001; Siwabessy, 2001). In addition, a rough seabed surface causes the echo to decay slowly in the decay phase, whereas it decays rapidly on a flat surface (Boulton and Wyness, 2001; Penrose et al., 2005). In this study, shallow sand and rubble with dense structures and compositions produced sharp and narrow echo envelope curves. In contrast, soft-bottom types, such as soft corals, produced broad echo envelope curves. The results of this study also show differences in the echo envelope curve between massive corals (CM) and branching corals (ACB and ACT), especially the shape of the curve at the end of the curve in the decay phase. The difference lies in the position of the broadening curve, with the decay phase curve of massive corals (CM) tending to broaden at the top (near the top of the curve), while the decay phase curve of branching corals (ACB and ACT) broadens at the bottom. The difference in the shape of the echo envelope curve between the sandy bottom type, the hard corals (massive and branched) and the soft corals is clearly visible in the first echo (see Figure 6).

In this study, the sandy bottom type consistently showed acoustic backscattering with a high bottom peak energy in all three echoes of the seabed. The shallow seabed type reflects acoustic echoes maximally in the first echo; therefore, the energy of the second and third bottom peaks (BP2 and BP3) is still relatively high. In contrast, rough seabed or branching coral types scatter the reflected echoes in all directions and irregularly, so that more energy is lost in the second and third bottom peaks (BP2 and BP3). The energy of the bottom peak in the first echo is higher due to the direct reflectivity of the seabed surface (Penrose et al., 2005) and is also influenced by echoes from below the surface (Chivers et al., 1990). According to Lurton (2002), low seabed roughness leads to a relatively low specular component and low scattering. In contrast, high roughness weakens the specular component and increases scattering in all directions. As a result, the energy of the third echo of the branching hard coral species (ACB and ACT) is very low and almost undetectable due to the high-energy scattering in the previous two echoes. According to Hamilton (2001), the energies of the second and subsequent echo are sometimes not detected in certain cases, such as very rough seabed structures, rocky seabeds and undulating sandy seabed surfaces. The amount of bottom peak energy between different seabed types is also closely related to the structure and composition beneath the seabed surface through which the acoustic waves pass. In general, the composition of the seabed (e.g. sand or mud) is different between the surface and below the seabed surface (to a certain depth), with a denser granular composition below the surface to a certain depth, resulting in a higher acoustic backscatter energy (as energy bottom peak) (Pujiyati et al., 2019).

The acoustic energy in the attack phase (AttackSv) can describe the degree of hardness caused mainly by the seabed surface, while the decay energy (DecaySv) describes the degree of roughness of the seabed caused by backscattering propagating from the substrate volume (Burczynski, 1999; Balk and Lindem, 2015). The results of this study show significant differences in acoustic backscatter in the attack and decay phases of different types of seabed. Sand consistently has a higher AttackSv energy than the other seabed types in all three seabed echoes. This indicates that the sand substrate in this study has a structure and composition of sand grains on and below the surface that tend to be denser and harder. However, the DecaySv energy of the sandy bottom type tended to be lower than that of the massive hard coral (CM) in all three seabed reflection echoes. Tail length and acoustic energy during acoustic wave propagation can be used to directly measure the acoustic roughness of the seabed surface (Penrose et al., 2005).

In this study, significant differences in DecaySv energy were found between various types of hard corals. This difference is visible in the echo envelope curve (decay phase in the first echo; Figure 5). Although both are hard corals, they significantly differ in the acoustic energy during the decay phase. The CM forms a broad curve of the decay phase near the echo peak, so that the decay samples along three times the acoustic wavelength have high values. In contrast, ACT and ACB form a broad decay phase curve at the bottom, so that the decay samples along three times the acoustic wavelength have low values. Similarly, SA and RB have narrow and steep decay phase curves. Thus, there is a significant difference in DecaySv1 energy between massive corals which have many protrusions on their surface (may be rough) and branching corals, as well as differences from the flat seabed type. Similarly, the same seabed with different surface properties produces different acoustic backscatter energies. In this study, for example, we compared bare sand with the presence of seagrass growth on the sandy bottom. The presence of seagrass vegetation affects the acoustic backscatter energy. According to Siwabessy (2001), the energy reflected from vegetation can give an indication of the hardness of the seabed if vegetation growth is present on the surface of the seabed. In this study, seagrass vegetation above the seabed surface lowers the energy of bottom detection.

Overall, Sonar5-Pro software provides a convenient way to quantify acoustic backscatter energy from SBES instrument recordings, including various acoustic parameters in the first to third echoes. The results of this study show that there are significant differences in the acoustic backscatter energy (BD, BP1, AttackSv1, DecaySv1, AttDecSv1, BP2,

AttackSv2, DecaySv2, AttDecSv2, BP3, AttackSv3, DecaySv3 and AttDecSv3) of eight types of seabeds (sand, sand and seagrass, four types of hard corals, rubble and soft corals) investigated. However, some of them showed similar acoustic backscattering. The acoustic backscatter decreases in the second and third echoes. The relatively flat sand type has a higher peak base energy and AttackSv (indicating hardness level) than the other seabed types. However, this differs from the DecaySv energy (indicating the degree of roughness), while massive coral (CM) has a higher DecaySv energy in the first, second and third echoes. This study also found differences in the characteristics of acoustic wave propagation patterns between different types of seabeds, which are shown in the echo envelope. The relatively flat sandy bottom forms a sharper and narrower curve, while hard and soft corals form broader curves in the decay phase. In particular, massive corals form a broad curve in the decay phase near the top of the echo, while branching corals form a broad curve at the base of the decay phase.

The differences in acoustic backscatter energy from different types of seabeds identified in this study have important implications for spatial mapping studies of seabed benthos, particularly coral reefs and submerged aquatic vegetation, which are habitats for marine benthic organisms. Based on the results of this study, thirteen acoustic parameters in the first to third echoes showed predominantly significant differences between the seabeds studied. This suggests that these acoustic parameters can produce accurate maps when used as input parameters for classification and mapping. As the results of our recent study show, the use of seven acoustic parameters (BD, BP1, AttackSv1, DecaySv1, AttDecSv1, AttDecSv2 and AttDecSv3) in combination with depth data resulted in more accurate benthic maps (coral, seagrass and sand) than the use of only two main parameters from SBES applied to the RoxAnn system (Hamuna et al., 2024). Similarly, the results of the study by Shao et al. (2021) yielded more accurate benthic maps (algal cover and barren seabed) using six acoustic parameters (including depth) compared to two acoustic parameters in the RoxAnn system.

## **ACKNOWLEDGEMENTS**

This research was funded through the Indonesian Education Scholarship (Beasiswa Pendidikan Indonesia; BPI ID: 202101120886). Therefore, the authors would like to express their deepest gratitude to the Center for Higher Education Funding and Assessment (Pusat Pembiayaan dan Asesmen Pendidikan Tinggi; PPAPT) at the Ministry of Higher Education, Science, and Technology of the Republic of Indonesia, and the Indonesia Endowment Funds for Education (Lembaga Pengelola Dana Pendidikan; LPDP).

## **CONFLICT OF INTEREST**

The authors declared no potential conflicts of interest with respect to the research and publication of this article.

## REFERENCES

- Amiri-Simkooei, A.R., Koop, L., van der Reijden, K.J., Snellen, M. & Simons, D.G., (2019). Seafloor characterization using multibeam echosounder backscatter data: Methodology and results in the North Sea. *Geosciences*, 9(7), pp. 292. Available at: <http://dx.doi.org/10.3390/geosciences9070292>.
- Anderson, J.T., Holliday, D.V., Kloser, R., Reid, D.G. & Simard, Y., (2008). Acoustic seabed classification: current practice and future directions. *ICES Journal of Marine Science*, 65, pp. 1004-1011. Available at: <http://dx.doi.org/10.1093/icesjms/fsn061>.
- Balk, H. & Lindem, T., (2015). *Sonar4 and Sonar5-Pro Post Processing Systems, Operator Manual Version 6.0.3*. Oslo Norway: University of Oslo.
- Balk, H., Lindem, T. & Sánchez-Carnero, N., (2011). *Sonar4 and Sonar5 post processing systems. Operator manual version 6.0.1. Extension for Seabed Classification Tool*.
- Bejarano, S., Mumby, P.J., Hedley, J.D. & Sotharan, I., (2010). Combining optical and acoustic data to enhance the detection of Caribbean forereef habitats. *Remote Sensing of Environment*, 114, pp. 2768-2778. Available at: <http://dx.doi.org/10.1016/j.rse.2010.06.012>.
- Boulton, B. & Wyness, R., (2001). *Sangachal Seabed Mapping Survey: Annual Report ERT 1610*. London: BP.
- Brown, J.C., Beaudoin, J., Brissette, M. & Gazzola, V., (2019). Multispectral multibeam echosounder backscatter as a tool for improved seafloor characterization. *Geoscience*, 9(3), pp. 126-143. Available at: <http://dx.doi.org/10.3390/geosciences9030126>.
- Burczynski, J., (1999). *Bottom Classification*. BioSonics Inc. Available at: [http://www.biosonicsinc.com/doc\\_library/docs/bottom\\_classification.pdf](http://www.biosonicsinc.com/doc_library/docs/bottom_classification.pdf). accessed on: August 8, 2022.
- Chivers, R.C., Emerson, N. & Burns, D., (1990). New acoustic processing for underwater surveying. *Hydrology Journal*, 56, pp. 9-17.
- Chotiros, N.P., (2017). *Acoustics of the Seabed as a Poroelastic Medium*. New York: Springer Cham. Available at: <http://dx.doi.org/10.1007/978-3-319-14277-7>.
- Demer, D.A., Cutter, G.R., Renfree, J.S. & Butler, J.L., (2009). A statistical-spectral method for echo classification. *ICES Journal of Marine Science*, 66, pp. 1081-1090. Available at: <http://dx.doi.org/10.1093/icesjms/fsp054>.
- Elson, L., Manik, H.M., Hestirianto, T. & Pujiyati, S., (2022). Kuantifikasi hambur balik akustik dasar laut menggunakan scientific single beam echosounder. *Jurnal Ilmu dan Teknologi Kelautan*, 14(1), pp. 15-29. Available at: <http://dx.doi.org/10.29244/jitkt.v14i1.37184>.
- Fauziyah, F., Purwiyanto, A.I.S., Agustriani, F., Putri, W.A.E., Liyani, M., Aryawati, R., Ningsih, E.N. & Suteja, Y., (2020). Detection of bottom substrate type using single-beam echo sounder backscatter: a case study in the east coastal of Banyuasin. *IOP Conference Series: Earth and Environmental Science*, 404, pp. 012004. Available at: <http://dx.doi.org/10.1088/1755-1315/404/1/012004>.
- Fonseca, L. & Mayer, L., (2007). Remote estimation of surficial seafloor properties through the application angular analysis to multibeam sonar data. *Marine Geophysical Researches*, 28, pp. 119-126. Available at: <http://dx.doi.org/10.1007/s11001-007-9019-4>.
- Freitas, R., Rodrigues, A.M., Morris, E., Perez-Llorens, J.L. & Quintino, V., (2008). Single-beam acoustic ground discrimination of shallow water habitats: 50 kHz or 200 kHz frequency survey? *Estuarine, Coastal and Shelf Science*, 78, pp. 613-622. Available at: <http://dx.doi.org/10.1016/j.ecss.2008.02.007>.
- Hamilton, L.J., (2001). *Acoustics Seabed Classification System*. DSTO Technical Note, DSTO-TN-0401. Victoria (AU): DSTO Aeronautical and Maritime Research Laboratory. Available at: <http://www.dsto.defence.gov.au/corporate/reports/DSTO-TN-0401.pdf>. accessed on: December 12, 2023.
- Hamouda, A., Soliman, Kh., El-Gharabawy, S. & Nassar, M., (2019). Comparative study between acoustic signals and images for detecting seabed features. *Egyptian Journal of Aquatic Research*, 45, pp. 145-151. Available at: <http://dx.doi.org/10.1016/j.ejar.2019.03.002>.
- Hamouda, A.Z. & Abdel-Salam, K.M., (2010). Acoustic seabed classification of marine habitats: studies in the Abu-Qir Bay, Egypt. *Journal of Oceanography and Marine Science*, 1(1), pp. 11-22.
- Hamuna, B., Dimara, L., Pujiyati, S. & Natih, N.M.N., (2018). Correlation of substrate fraction percentage with acoustic backscattering strength from single beam echosounder detection. *AAAL Bioflux*, 11(4), pp. 1343-1351.
- Hamuna, B., Pujiyati, S. & Hestirianto, T., (2014). Karakterisasi pantulan akustik karang menggunakan echosounder single beam. *Jurnal Integrasi*, 6(2), pp. 129-133.
- Hamuna, B., Pujiyati, S., Gaol, J.L. & Hestirianto, T., (2024). Classification and prediction of benthic habitat based on scientific echosounder data: application of machine learning algorithms. *Applied Computer Science*, 20(4), pp. 100-116. Available at: <https://doi.org/10.35784/acs-2024-42>.
- Hilgert, S., Sotiri, K. & Fuchs, S., (2019). Advanced assessment of sediment characteristics based on rheological and hydro acoustic measurements in a Brazilian reservoir. In: *E-proceedings of the 38th IAHR World Congress September 1-6, 2019, Panama City, Panama*; pp. 61-70. Available at: <http://dx.doi.org/10.3850/38WC092019-0616>.
- Hilgert, S., Wagner, A., Kiemle, L. & Fuchs, S., (2016). Investigation of echo sounding parameters for the characterisation of bottom sediments in a sub-tropical reservoir. *Advances in Oceanography and Limnology*, 7, pp. 5623. Available at: <http://dx.doi.org/10.4081/aiol.2016.5623>.

- Huang, Z., Siwabessy, J., Cheng, H. & Nichol, S., (2018). Using multibeam backscatter data to investigate sediment-acoustic relationships. *Journal of Geophysical Research: Oceans*, 123(7), pp. 4649-4665. Available at: <http://dx.doi.org/10.1029/2017JC013638>.
- Lee, W.S. & Lin, C.Y., (2018). Mapping of tropical marine benthic habitat: Hydroacoustic classification of coral reefs environment using single-beam (RoxAnn™) system. *Continental Shelf Research*, 170, pp. 1-10. Available at: <http://dx.doi.org/10.1016/j.csr.2018.09.012>.
- Lumivero, (2024). XLSTAT Statistical and Data Analysis Solution. Available at: <https://www.xlstat.com/en>.
- Lurton, X., (2002). *An Introduction to Underwater Acoustics. Principles and Application*. London: Springer.
- Mamede, R., Rodrigues, A.M., Freitas, R. & Quintino, V., (2015). Single-beam acoustic variability associated with seabed habitats. *Journal of Sea Research*, 100, pp. 152-159. Available at: <http://dx.doi.org/10.1016/j.seares.2015.04.007>.
- Manik, H.M., (2012). Seabed identification and characterization using sonar. *Advances in acoustics and vibration*, 2012, pp. 532458. Available at: <http://dx.doi.org/10.1155/2012/532458>.
- Parnum, I., Siwabessy, J., Gavrilov, A. & Parsons, M., (2009). A comparison of single beam and multibeam sonar systems in seafloor habitat mapping. In: *Proc. 3rd Int. Conf. and Exhibition of Underwater Acoustic Measurements: Technologies & Results*, Nafplion, Greece; pp. 155-162.
- Penrose, J.D., Siwabessy, P.J.W., Gavrilov, A., Parnum, I., Hamilton, L.J., Bickers, A., Brooke, B., Ryan, D.A. & Kennedy, P., (2005). *Acoustics Techniques for Seabed Classification*. Technical Report 32. Australia: CRC for Coastal Zone Estuary and Waterway Management.
- Poulain, T., Argillier, C., Gevrey, M. & Guillard, J., (2011). Identifying lakebed nature: is it feasible with a combination of echosounder and Sonar5-pro? *Advances in Oceanography and Limnology*, 2, pp. 49-53. Available at: <http://dx.doi.org/10.1080/19475721.2011.565803>.
- Pujiyati, S., Natih, N.M.N., Hamuna, B. & Dimara, L., (2019). The value of acoustic backscattering in determining the integration thickness of the seabed in Yos Sudarso Bay Papua. *Journal of Applied Geospatial Information*, 3(2), pp. 240-243. Available at: <http://dx.doi.org/10.30871/jagi.v3i2.1605>.
- Shao, H., Kiyomoto, S., Kawauchi, Y., Kadota, T., Nakagawa, M., Yoshimura, T., Yamada, H., Acker, T. & Moore, B., (2021). Classification of various algae canopy, algae turf, and barren seafloor types using a scientific echosounder and machine learning analysis. *Estuarine, Coastal and Shelf Science*, 255, pp. 107362. Available at: <http://dx.doi.org/10.1016/j.ecss.2021.107362>.
- Simrad, (2012). *Installation Manual: Simrad EK15 Multi-purpose Scientific Echosounder*. Available at: <http://www.simrad.com/ek15>. accessed on: January 2, 2022.
- Siwabessy, P.J.W., (2001). *An Investigation of The Relationship Between Seabed Type and Benthic and Benthic-Pelagic Biota Using Acoustic Techniques*. Australia: The Curtin University of Technology.
- Solikin, S., Manik, H.M., Pujiyati, S. & Susilohadi, S., (2018). Measurement of bottom backscattering strength using single-beam echosounder. *IOP Conf. Series: Journal of Physics: Conf. Series*, 1075, pp. 012036. Available at: <http://dx.doi.org/10.1088/1742-6596/1075/1/012036>.
- Thermo, P.D., Pace, N.G. & Al-Hamdani, Z.K.S., (1988). Laboratory measurements of backscattering from marine sediments. *The Journal of the Acoustical Society of America*, 84, pp. 303-309. Available at: <http://dx.doi.org/10.1121/1.396985>.
- Urick, R.J., (1983). *Principles of Underwater Sound*. 3rd Edition. New York: McGraw-Hill Publishing.
- Yusop, M.S.M., Razali, M.N., Tarmizi, N.Md., Yolhamid, M.N.A.G., Azzeri, M.N. & Rahman, A.H.A., (2021). Acoustic approach to determining seabed substrates distribution at Mandi Darah Island, Sabah. *Transactions on Maritime Science*, 2, pp. 374-382. Available at: <http://dx.doi.org/10.7225/toms.v10.n02.007>.
- Zhang, H., Wang, C.Y., Wu, J.M., Du, H., Wei, Q.W. & Kang, M., (2016). Physical habitat assessment of a remaining high-biodiversity reach of the upper Yangtze River, China. *Applied Ecology and Environmental Research*, 14(1), pp. 129-143. Available at: [http://dx.doi.org/10.15666/aeer/1401\\_129143](http://dx.doi.org/10.15666/aeer/1401_129143).